

Semester Project

Kinks

prepared by
David Maibach

at the Department of Physics,
Swiss Federal Institute of Technology (ETH) Zurich

Supervision

Dr. Valentin Hirschi

Organised by

Prof. Matthias Gaberdiel

May 13, 2020

Abstract

In this work we analyze the stable non-minimal energy solutions of a 1 dimensional, real scalar field theories with non-trivial vacuum structure, called kinks. The analysis will focus on classical and relativistic solutions for two particular potentials: the ϕ^4 - and the Sine-Gordon potential. Furthermore, we will discuss an approach on how to simulate these solutions and their dynamics numerically.

Contents

1	Introduction	2
2	Topology and vacuum structure	3
3	ϕ^4 kinks	5
3.1	Single kink/antikink solution	6
3.2	Multi-kink interactions	8
4	Sine-Gordon model	10
4.1	Single kinks	10
4.2	Multi-kink solutions and Bäcklund transformation	12
4.3	Thirring-Model	16
5	Simulations	18
5.1	General approach	18
5.2	Multi-kink interaction	19
6	Conclusion	21
A	Topology and vacuum manifolds	22

1 Introduction

In this work we will investigate the behavior of stable vacuum solutions with non trivial boundary conditions identified by topological invariants in the ϕ^4 -theory and the Sine-Gordon model in close analogy to section 5.1 to 5.3 of “Topological solitons” by P. Manton and P. Sutcliffe [1]. Moreover, we will support this investigation with numerical work on the dynamics of kinks especially of multi-kink scenarios where there is no analytical solution in form of differentiable functions. The motivation to do so is manifold:

Topological solitons play an important in many fields in physics such as condensed matter physics, cosmology, nuclear physics and quantum field theory. The simplest form of solitons, kinks, find applications not only in classical wave mechanics but their scattering and decay processes in the quantum regime are of great interest for physicist studying false vacuum decay in inflationary models, phase transitions and baryogenesis beyond others. Kinks embedded in higher dimensions are, therefore, a powerful concept to describe a variety of phenomena in theoretical physics as listed in the introduction of ref. [2]. It is also worth mentioning that the interpretation of soliton solutions as particles governed by classical equations yields interesting implications in the quantum regime. E.g. it is possible to think of a scenario in which two kinks scatter at relativistic speed and one of the kinks loses a fraction of its kinetic energy during the scattering process which results in radiation or elementary particles as it is described in section 1.1 of ref. [1]. Thus, the broad field of applications of solitons motivates to study more deeply their dynamical behavior as well as their intrinsic vacuum structure.

This work starts with an general treatment of the topology and the vacuum structure of general 1-dimensional real scalar theories with non-trivial vacua in section 2. Next, in section 3, we discuss the structure of possible kink solutions in the ϕ^4 -theory and their interactions. The same procedure will be applied on the Sine-Gordon model in section 4. In section 5, we will present a possible approach to simulate the equations that govern the solitons behaviour, if such exists, for a general theory and we will discuss results for both scalar field potentials. Finally, in section 6 we give a brief summary of the results and highlight critical insights.

2 Topology and vacuum structure

As stated in the introduction, in this work we consider general 1-dimensional, real scalar field theories, for which the Lagrangian reads:

$$\mathcal{L} = \frac{1}{2} \partial_\mu \phi \partial^\mu \phi - U(\phi).$$

where $U(\phi)$ is a non-negative function. The equation of motion can be derived using the Euler-Lagrange equation:

$$\partial_\mu \partial^\mu \phi + \frac{dU}{d\phi} = 0. \quad (1)$$

Since U is non-negative and an addition of a constant does not change the field equations, we can simply set U_{min} to be zero without loss of generality.

By splitting the Lagrangian into kinetic and potential energy $\mathcal{L} = T - V$, we can make the identification

$$T = \frac{1}{2} \int_{-\infty}^{+\infty} \dot{\phi}^2 dx, \quad V = \int_{-\infty}^{+\infty} \left(\frac{1}{2} \phi'^2 + U(\phi) \right) dx,$$

where $\dot{\phi} = \frac{d\phi}{dt}$ and $\phi' = \frac{d\phi}{dx}$.

For the existence of solitons, or more accurately kinks, the arbitrary potential term U that we introduced must satisfy certain criteria in the sense that the vacuum manifold \mathcal{V} defined by the field configurations that minimize U must be non-trivial. Define

$$\mathcal{V} = \{ \phi_0, \text{ s. t. } U(\phi_0) = U_{min} \},$$

where, as argued before, U_{min} can be set to zero. In addition, we require that on the vacuum manifold the total energy is minimal, namely zero, so that $\dot{\phi}_0 = \phi'_0 = 0$ on \mathcal{V} .

To characterize the vacuum manifold further and, especially, identify what makes it non-trivial we will use the notations and the tools of algebraic topology which are briefly summarized in the appendix A and elaborated in more detail in section 3 and 4 of [1].

Using this knowledge, the criteria for the existence of topological solitons in the case of the 1-dimensional real scalar field can be written as $\pi_0(\mathcal{V}) \neq 0$. In words, we want our vacuum manifold to allow ϕ_0 in distinct regions in space to lay in (at least) two topologically distinct points in \mathcal{V} . As we only want to consider finite energy field configuration we have to demand finite energy boundary conditions meaning that $\mathcal{E}(x) \xrightarrow{x \rightarrow \pm\infty} 0$, where $\mathcal{E}(x)$ is the total energy density of our field configuration depending on x . Since these are the only restrictions on our field in the sense that for finite space there is no limitation on the functional form of the energy density except that it must be finite, we can characterize it topologically via an element $(\phi_-, \phi_+) \in \pi_0(\mathcal{V}) \times \pi_0(\mathcal{V})$ where $\phi_\pm = \lim_{x \rightarrow \pm\infty} \phi(x)$. This topological data (ϕ_-, ϕ_+) can in general be divided into two cases:

If $\phi_- = \phi_+$ the field at finite points can be continuously deformed to the constant value $\phi(x) = \phi_+$ and the result will be a zero energy field configuration. If, contrary to that, $\phi_- \neq \phi_+$, then continuously deforming one vacuum into the other would force the field to leave the vacuum manifold for spatial infinity (+ or -) and, consequently, yield finite energy density along that region since $\phi_\pm \notin \mathcal{V}$. Hence, there is no such transition possible under the condition of keeping the energy finite. This is the root of the stability of a kink solution in the regime of solutions with such asymmetrical topological configuration. It follows that this stability also holds for dynamical kink solutions since time evolution is an example of a continuous deformation leaving energy finite.

Since $\phi_- \neq \phi_+$ describes a non-zero energy solution we want to investigate the minimal energy this type of solution can acquire and express it in terms of the topological data (ϕ_-, ϕ_+) . Starting from

$$\left(\frac{1}{\sqrt{2}}\phi' \pm \sqrt{U(\phi)}\right)^2 \geq 0, \quad (2)$$

we can integrate over space and expand:

$$\int_{-\infty}^{+\infty} \left(\frac{1}{2}\phi'^2 + U(\phi)\right) dx \geq \pm \int_{-\infty}^{+\infty} \sqrt{2U(\phi)}\phi' dx \quad (3)$$

$$\Rightarrow E \geq \left| \int_{-\infty}^{+\infty} \sqrt{2U(\phi)}\phi' dx \right| = \left| \int_{\phi_-}^{\phi_+} \sqrt{2U(\phi)} d\phi \right| = |W(\phi_+) - W(\phi_-)|. \quad (4)$$

The first term in equation (3) can be identified as the potential energy. Since $T \geq 0$ we can write this term as the total energy E . In order to arrive at equation (4) we take the absolute value and rewrite $\phi' = \frac{d\phi}{dx}$. Changing the boundaries of the integration accordingly we arrive at a lower bound for the energy depending only on (ϕ_-, ϕ_+) . Since $U(\phi) \geq 0$ for every possible value of ϕ , we can introduce a super-potential W defined as $U = \frac{1}{2}(\frac{dW}{d\phi})^2$ which yields the last term in (4). This expression of the lower energy bound in terms of the topological data is known as the Bogomolny bound and can also be generalized to higher dimensional solitons.

This Bogomolny bounds are especially useful in order to derive analytical functions characterizing kink solutions. To do so, we look at the ϕ that attain equality in the Bogomolny bound. From (2), we find that the defining equation for the kink is given by

$$\phi' = \pm \sqrt{2U(\phi)}, \quad (5)$$

where the $+$ describes the kink and $-$ the antikink. An illustration of the different functional forms will be given in the next sections where we consider specific potentials.

Per definition, solutions of the Bogomolny bounds such as (5) are global minima of the energy within a topological class of fields. Naturally, they are static solutions and, hence, satisfy the static equation of motion (1). Simply applying a Lorentz boost to the obtained solution will make it dynamical. Note here that the speed of light in the units chosen in this work is 1, hence, the kink can only be boosted with $-1 < v < 1$.

So far, this concludes setting up the mindset for characterizing kink solitons in the most general way. What follows is an introductory example of the simplest model with kinks before discussing a more involved model with a richer vacuum structure.

3 ϕ^4 kinks

In the ϕ^4 -theory the potential is polynomial in ϕ^2 up to second order:

$$U(\phi) = \mu + \nu\phi^2 + \lambda\phi^4.$$

Demanding kink solutions and an energy bounded from below, we can adapt the constants λ, μ, ν in such a way that we get a potential of the form of the blue line in figure 1 with $\pi_0(\mathcal{V}) = \mathbb{Z}_2$. To do so we have to chose $\lambda > 0$ to bound the energy from below. Moreover, we take $\nu < 0$, otherwise U would have a unique minimum at $\phi = 0$, thus excluding, per definition, kink solutions. A convenient choice is to define $\nu = -2m^2\lambda$ and $\mu = \lambda m^4$ with m being a positive real constant such that

$$U(\phi) = \lambda(m^2 - \phi^2)^2.$$

Such a choice also ensures that $U_{min} = 0$.

We illustrate the potential in figure 1. It is worth mentioning that a popular application of kinks is indeed the kink decay. If we switch to the quantum regime for this example and imagine a potential such as the orange line in figure 1, assuming ϕ_- lays on the left and ϕ_+ on the right minimum, there is a possibility of quantum tunneling towards the solution $\phi(x) = \phi_+$.

Back to the classical regime, we now have two degenerated global minima $\phi = \pm m$ (blue line in figure 1) and the equation of motion is then given by

$$\partial_\mu \partial^\mu \phi - 4\lambda(m^2 - \phi^2)\phi = 0. \quad (6)$$

It is possible to capture the topological content of a field configuration with an integer number:

$$N = \frac{\phi_+ - \phi_-}{2m}.$$

This defines a topological charge with the possible values $N \in \{-1, 0, 1\}$, where $+1$ is the kink and -1 the antikink. $N = 0$ can be achieved by an kink-antikink solution as well as with the trivial vacuum. In principle, however, an arbitrary number of alternating kink-antikink pairs is possible. Treating the topological charge as a conserved quantity of the system we can construct an associated topological current

$$j^\mu = \frac{1}{2m} \epsilon^{\mu\nu} \partial_\nu \phi. \quad (7)$$

Then N is recovered in the following way:

$$N = \int_{-\infty}^{\infty} j^0 dx = \frac{1}{2m} \int_{-\infty}^{\infty} \epsilon^{01} \partial_1 \phi dx = \frac{1}{2m} \int_{-\infty}^{\infty} \frac{\partial \phi}{\partial x} dx = \frac{1}{2m} \int_{\phi_-}^{\phi_+} d\phi = \frac{\phi_+ - \phi_-}{2m}.$$

This current appears to be very different from the Noether currents of classical mechanics. In fact the topological current j^μ is always conserved, independent of the equation of motion (6)

$$\partial_\mu j^\mu = \frac{1}{2m} \epsilon^{\mu\nu} \partial_\mu \partial_\nu \phi = 0,$$

since the two derivatives applied on ϕ form a symmetric term while the ϵ -tensor is totally anti-symmetric. Hence, the current is per construction conserved. These are not the only differences with respect to the Noether current. It is evident that j^0 contains no canonical

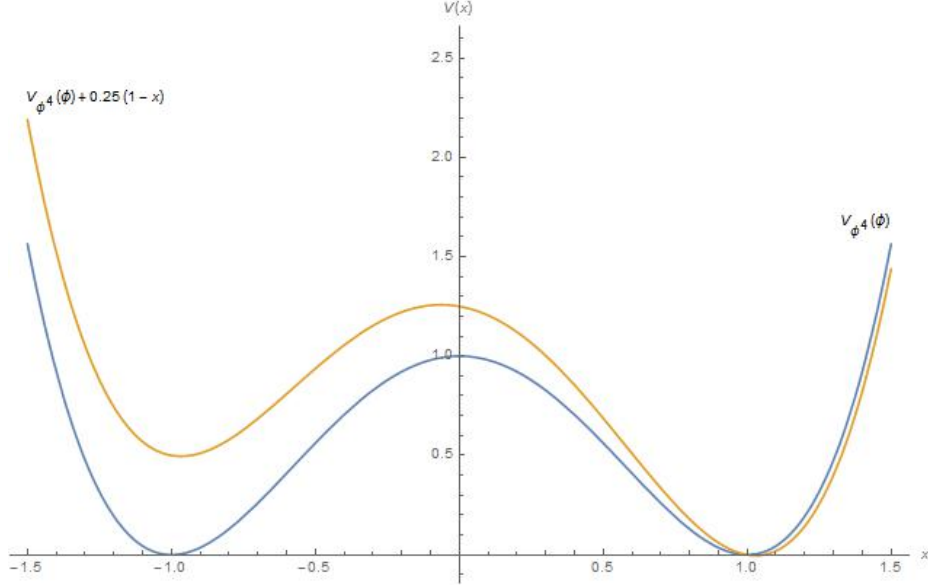


Figure 1: Potential V_{ϕ^4} of the ϕ^4 -theory with $\mu = 1$, $\nu = -2$, $\lambda = 1$ (blue) and the same potential with an additive term $V_{\phi^4}(\phi) + 0.25(1 - \phi)$ (orange) as a function of ϕ . In the quantum regime, a field configuration laying in the l.h.s. of the latter potential would eventually tunnel into the global minimum.

momenta, hence its Poisson brackets with coordinates vanishes. Thus, j^0 does not generate any spacial symmetries [3].

Perhaps the most outstanding fact about the topological current and its associated charge is that, although working in the classical regime, the charge takes discrete values. For now we leave this statement as is and postpone further discussions to the section treating the Sine-Gordon model. This much richer model indeed allows the topological charge N to span all natural numbers.

3.1 Single kink/antikink solution

We first investigate kinks in this model by demanding minimal energy static solutions. As described before, a dynamical solution can then simply be obtained by applying a Lorentz boost to the static one.

A static kink solution is given by a field configuration attaining equality in the Bogomolny bound. Hence, we want to take a look at the lower energy bound:

$$\begin{aligned}
 E &\geq \left| \int_{\phi_-}^{\phi_+} \sqrt{2U(\phi)} d\phi \right| = \left| \int_{\phi_-}^{\phi_+} \sqrt{2\lambda}(m^2 - \phi^2) d\phi \right| = \left| \sqrt{2\lambda} \left[m^2\phi - \frac{1}{3}\phi^3 \right]_{\phi_-}^{\phi_+} \right| \\
 &= \sqrt{2\lambda} \left| \left[m^2\phi - \frac{1}{3}\phi^3 \right]_{\mp m}^{\pm m} \right| = \sqrt{2\lambda} \frac{4}{3} |N| m^3.
 \end{aligned} \tag{8}$$

The lower bound $E \geq \sqrt{2\lambda} \frac{4}{3} |N| m^3$ holds for kinks and antikinks.

Attaining equality in the Bogomolny bound gives the defining equation

$$\phi' = \pm \sqrt{2U(\phi)} = \pm \sqrt{2\lambda}(m^2 - \phi^2),$$

where again the $-$ sign resembles the antikink and the $+$ sign the kink. Taking this equation

we can integrate:

$$\begin{aligned}
\frac{d\phi}{dx} &= \sqrt{2\lambda}(m^2 - \phi^2) \\
\Rightarrow \frac{d\phi}{(m^2 - \phi^2)} &= \sqrt{2\lambda}dx \\
\Rightarrow \frac{1}{m} \operatorname{artanh}\left(\frac{\phi}{m}\right) &= \sqrt{2\lambda}(x - a) \\
\Rightarrow \phi(x) &= m \tanh(\sqrt{2\lambda}m(x - a)).
\end{aligned} \tag{9}$$

Equation (3) finally gives us the analytical function for a static kink in the ϕ^4 -theory. The parameter a is an integration constant and can be identified as the position of the kink. This becomes more clear looking at the energy density of the static kink

$$E = \int_{-\infty}^{\infty} \mathcal{E} dx = \int_{-\infty}^{\infty} \frac{1}{2} \phi'^2 + \lambda(m^2 - \phi^2)^2 dx,$$

where the functional form of ϕ can be inserted to get

$$\begin{aligned}
E &= \int_{-\infty}^{\infty} \frac{1}{2} \left(\sqrt{2\lambda}m^2 \operatorname{sech}^2(\sqrt{2\lambda}m[x - a]) \right)^2 + \int_{-\infty}^{\infty} \lambda \left(m^2 - m^2 \tanh^2(\sqrt{2\lambda}m[x - a]) \right)^2 \\
&= \int_{-\infty}^{\infty} 2\lambda m^4 \operatorname{sech}^4(\sqrt{2\lambda}m(x - a)) dx.
\end{aligned} \tag{10}$$

In the last equality we used $\cosh^2 x - \sinh^2 x = 1$.

The identification $\mathcal{E} = 2\lambda m^4 \operatorname{sech}^4(\sqrt{2\lambda}m(x - a))$ once again indicates that a is the position of the kink since its energy density is equally distributed around $x = a$, being maximal exactly in that point (see figure 2). Note the fact that the energy density is distributed over a finite space is also indicative of the particle character of kink solutions. In addition, we can also interpret the lower energy bound of the kink to be equal to rest mass M , namely $M \equiv E_{\min} = \sqrt{2\lambda} \frac{4}{3} |N| m^3$.

The integration constant a , the position of the kink, is the only free parameter in this theory corresponding to translation invariance of the encountered Lagrangian. Thus, the moduli space for a 1-dimensional kink is $\mathcal{M}_1 = \mathbb{R}$.

Having found a general static solution we can now apply a Lorentz boost and obtain

$$\phi(t, x) = m \tanh(\sqrt{2\lambda}m\gamma(x - vt - a)),$$

where the velocity is bounded to $-1 < v < 1$ and $\gamma = \frac{1}{\sqrt{1-v^2}}$ is the Lorentz factor. In the non-relativistic limit $\gamma \rightarrow 1$ and for the dynamical kink solutions space and time derivative are proportional:

$$\dot{\phi} = -v\sqrt{2\lambda}m^2 \tanh(\sqrt{2\lambda}m(x - vt - a)) = -v \cdot \phi' = -v \cdot \left(\sqrt{2\lambda}m^2 \tanh(\sqrt{2\lambda}m(x - vt - a)) \right).$$

The kinetic energy can then be written as

$$T = \frac{1}{2} \int_{-\infty}^{\infty} \dot{\phi}^2 dx = \frac{1}{2} v^2 \int_{-\infty}^{\infty} \phi'^2 dx = \frac{1}{2} M v^2,$$

where in the last equation we used the virial theorem $\frac{1}{2} \int_{-\infty}^{\infty} \phi'^2 dx = \int_{-\infty}^{\infty} U(\phi) dx$ to write

$$\int_{-\infty}^{\infty} \phi'^2 dx = \frac{1}{2} \int_{-\infty}^{\infty} \phi'^2 dx + \frac{1}{2} \int_{-\infty}^{\infty} U(\phi) dx = M,$$

which equals the rest mass M of the kink shown in equation (8).

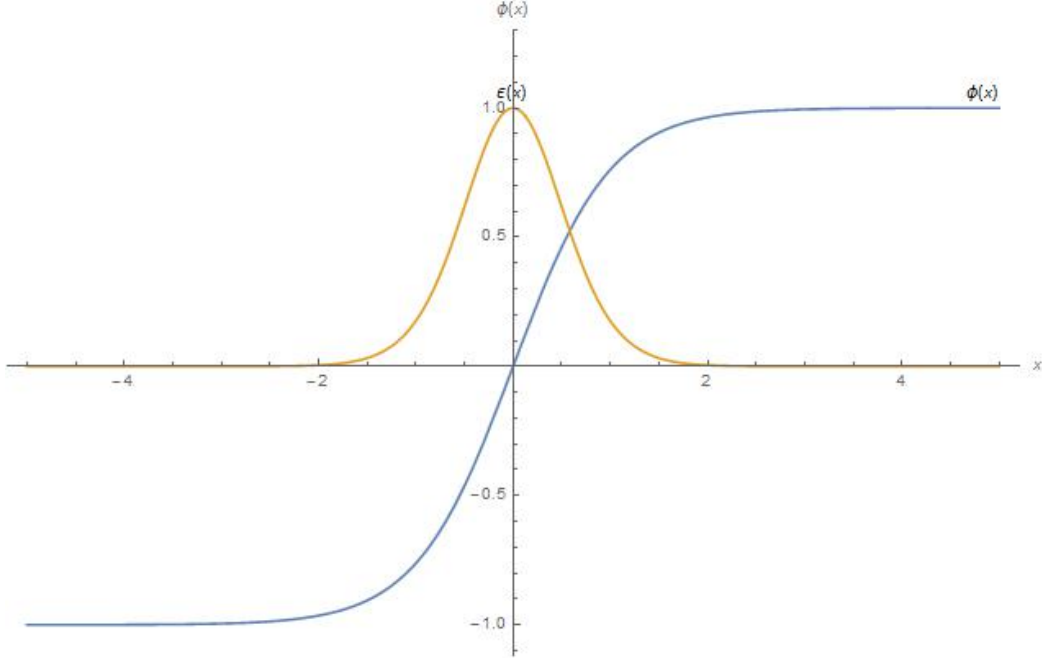


Figure 2: ϕ^4 kink with $m = 1$, $\lambda = \frac{1}{2}$ (blue) and its energy density (orange) as a function over space x . The peak in the energy density $\epsilon(x)$ corresponds to the kinks location in space.

3.2 Multi-kink interactions

To conclude this section about the ϕ^4 -theory, we now want to consider multi-kink solutions and investigate their interactions.

A kink-antikink configuration in the ϕ^4 -model has a topological charge $N = 0$ (if there is just one of each). Note that the configuration kink-antikink-kink would have topological charge $N = 1$. We are interested in studying the dynamics of a kink-antikink solutions. Hence, we have to calculate the interaction energy. This can be done in various ways. In this section, the interaction energy follows from the force acting on what can effectively be considered as the kink particle, induced by the antikink. However, the dynamics are involving the whole field. In order to take into account the kinks particle character and calculate a force which acts on the kink induced by the antikink, we, thus, have to calculate the force for an interval including just the kink itself.

In classical field theory, the momentum of a real scalar field on an interval bounded from above by an arbitrary parameter b is given by

$$P = - \int_{-\infty}^b \dot{\phi} \phi' dx.$$

Describing a kink-antikink pair analytically can be done by simple superposition of the two single kink solutions with $N = 1$ and $N = -1$. Choosing $\lambda = \frac{1}{2}$ and $m = 1$

$$\phi(x) = \phi_1(x) + \phi_2(x) + 1 = -\tanh(x + a) + \tanh(x - a) + 1. \quad (11)$$

From equation (11) we know that at initial time $t = 0$ kink and antikink are separated by a distance $R = 2a$. Note also that the field is initially static, there is no initial velocity, however, the second derivative with respect to time of the field is not zero, i.e. the interaction force we are going to calculate in the following induces an acceleration.

Given this functional description of equation (11) we can calculate the change of the momentum in an interval that includes only one of the solitons. Thus, we choose $-a \ll b \ll a$ which simplifies the calculation:

$$F = \dot{P} = - \int_{-\infty}^b (\ddot{\phi}\phi' + \dot{\phi}\dot{\phi}')dx = - \int_{-\infty}^b \left((\phi'' - \frac{dU}{d\phi})\phi' + \dot{\phi}\dot{\phi}' \right) dx = \left[-\frac{1}{2}(\dot{\phi}^2 + \phi'^2) + U(\phi) \right]_{-\infty}^b.$$

In the second integral we used the field equation (1) and in the following equality, we use the fact that the terms $\phi''\phi'$, $\frac{dU}{d\phi}\frac{d\phi}{dx}$ and $\dot{\phi}\dot{\phi}'$ are total derivatives. Since finite energy boundary condition require the field to be in a vacuum configuration at spatial infinities, derivative terms and the potential at the boundaries vanish. Inserting the ansatz (11) and expanding around $1 + \phi_2 \approx 0$ (since $-a \ll b \ll a$) gives

$$F = \left[-\frac{1}{2}\phi_1'^2 - \phi_1'\phi_2' + U(\phi_1) + (1 + \phi_2)\frac{dU}{d\phi}(\phi_1) \right]_{-\infty}^b = [-\phi_1'\phi_2' + (1 + \phi_2)\phi_1'']_{-\infty}^b,$$

where the time derivatives vanish because we are considering the force on the initial time slice (and we want to end up with an asymptotic solution) and the term $-\frac{1}{2}\phi_1'^2 + U(\phi)$ evaluates to zeros since the antikink satisfies the Bogomolny bound (5). For the second equation again the equation of motion (1) is used. In order to evaluate the bounds, we have to remember that the field configuration under consideration has vanishing spatial derivatives at infinity. Thus, the lower bound evaluates to zero. The upper bound b is far away from both kinks. Expanding ϕ_1 and ϕ_2 to their asymptotic forms is then sufficient to calculate the upper bound. Inserting

$$\phi_1(x) \sim -1 + 2e^{-2(x+a)}, \quad \phi_2(x) \sim -1 + 2e^{2(x-a)}$$

into the expression for the force yields

$$\begin{aligned} F &= 4e^{-2(x+a)}4e^{2(x-a)} + (2e^{2(x-a)})8e^{-2(x+a)} \Big|_{x=b} \\ &= 32e^{-4a} = 32e^{-2R} = \frac{dE_{int}}{dR}. \end{aligned} \tag{12}$$

The expression (12) is independent of b , which is expected since it was just a parameter introduced for calculation purposes. The interaction energy, $E_{int} = -16e^{-2R}$, is negative and decreases with the separation parameter R . Thus, kink and antikink are subject to an attractive force. Note again that this calculation holds only in the limit of large separation since we made many approximations to simplify the calculations based on R being large. However, in section 5 we will refer to a numerical simulation allowing to explore exact evolution in all regimes. The results show that this approximation of the interaction force is in fact very good in its domain of applicability.

Having calculated most of the essential quantities in the ϕ^4 theory, we now want to investigate a richer model, namely the Sine-Gordon model.

4 Sine-Gordon model

In the ϕ^4 theory it is not possible to construct multi-kink solutions with $N > 1$. Solely kink-antikink pairs are possible. This changes in the Sine-Gordon model as it features a potential with infinitely many distinct global minima.

The Sine-Gordon Lagrangian density is given by

$$\mathcal{L} = \frac{1}{2} \partial_\mu \partial^\mu \phi - (1 - \cos \phi),$$

where we already considered a convenient parameter choice. In its most general form, the potential term would read $U(\phi) = \frac{\alpha}{\beta}(a - \cos \phi)$. Again, the field equation can be derived through the use of the Euler-Lagrange equation:

$$\partial_\mu \partial^\mu \phi + \sin \phi = 0.$$

The most distinguishing characteristic of the Sine-Gordon model compared to the ϕ^4 -theory is that the zero energy vacua are given by $\phi = 2\pi n$ with $n \in \mathbb{Z}$. Thus, $\pi_0(\mathcal{V} = \mathbb{Z})$. This implies also that the topological charge N based on the topological data (ϕ_+, ϕ_-) , where $\phi_\pm = \phi(\pm\infty)$, can take any value $N \in \mathbb{Z}$. Since the Lagrangian is invariant under transformations $\phi \rightarrow \phi \pm 2\pi$ we can as well set $\phi_- = 0$ without loss of generality.

$$N = \frac{\phi_+ - \phi_-}{2\pi} = \frac{1}{2\pi} \int_{-\infty}^{\infty} \phi' dx \in \mathbb{Z}.$$

Again, we can construct a similar current associated to this charge as in (7). We will discuss it later on in this section.

4.1 Single kinks

Looking at the Bogomolny bounds the rest mass of the kinks in the Sine-Gordon model can be identified as

$$\begin{aligned} E &\geq \int_{\phi_-}^{\phi_+} \left| \sqrt{2(1 - \cos \phi)} \right| d\phi = \int_0^{2\pi N} \left| \sqrt{2(1 - \cos^2 \frac{\phi}{2} + \sin^2 \frac{\phi}{2})} \right| d\phi = \int_0^{2\pi N} \left| 2 \sin \frac{\phi}{2} \right| d\phi \\ &= 4|N| \left[-\cos \frac{\phi}{2} \right]_0^{2\pi} = 8|N|, \end{aligned}$$

where we used the periodicity of the integrand and that the integration over the given interval is equivalent to integrating N -times over $[0, 2\pi]$. Attaining equality in the Bogomolny bound yields a defining equation that can be integrated in order to get an analytical solution for kinks in the Sine-Gordon model:

$$\begin{aligned} \frac{d\phi}{dx} &= \pm 2 \sin \frac{\phi}{2} \\ \Rightarrow \frac{d\phi}{\sin \frac{\phi}{2}} &= 2dx \\ \Rightarrow -2 \log(\cos \frac{\phi}{4}) + 2 \log(\sin \frac{\phi}{4}) &= 2(x - a) \\ \Rightarrow e^{-\log(\cos \frac{\phi}{4}) + \log(\sin \frac{\phi}{4})} &= e^{(x-a)} \\ \Rightarrow \frac{\sin \frac{\phi}{4}}{\cos \frac{\phi}{4}} &= e^{(x-a)} \\ \Rightarrow \phi(x) &= 4 \arctan(e^{(x-a)}). \end{aligned} \tag{13}$$

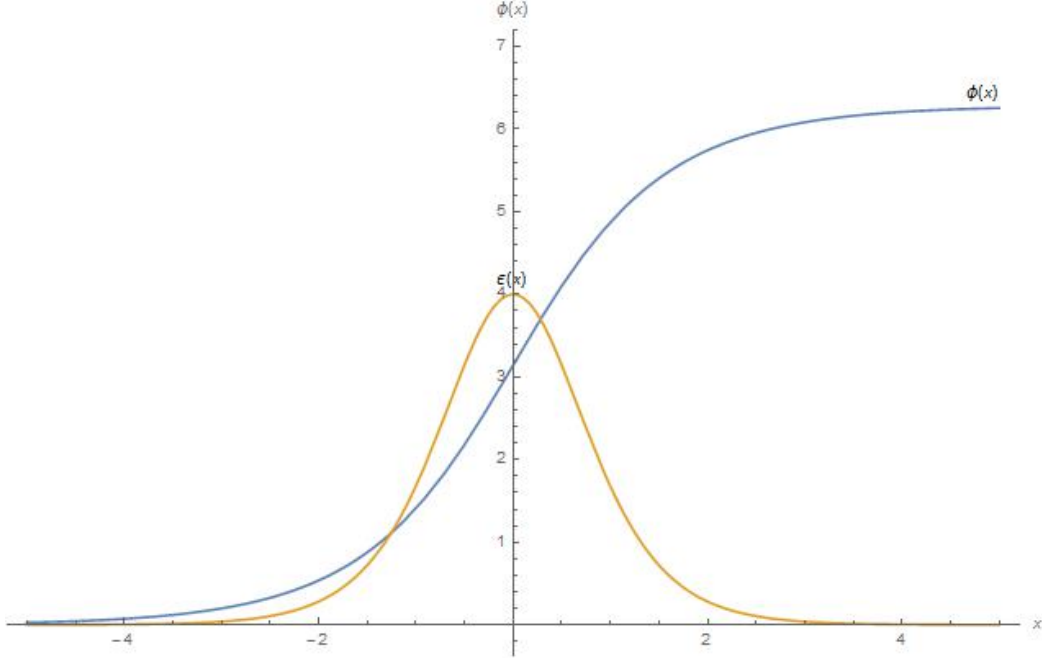


Figure 3: Sine-Gordon kink (blue) and its energy density (orange) as a function of space x . The peak in the energy density $\epsilon(x)$ corresponds to the kink's position in space.

In the first step, we choose the $+$ sign, hence, equation (13) describes a kink. Checking the limits of the function we get $\phi_- = 0$ and $\phi_+ = 2\pi$. Therefore, equation (13) gives an analytical expression for a single kink solution. The integration constant a is again the only free parameter and equals the position of the kink. Note that the antikink solution can be obtained by simply replacing $\phi \rightarrow -\phi$. In analogy to equation (10) the energy density in this model can be calculated to

$$\mathcal{E} = 4\text{sech}^2(x - a).$$

The energy density is maximal at $x = a$ and non-trivial only over a finite region, as shown in figure 3. This supports the interpretation of a kink as a particle localized at $x = a$.

As derived in equation (13), the general solution of the Bogomolny bound is a kink of topological charge $N = 1$. Analogously, this implies that there is no static solution with $N \neq 1$ or -1 . For two kinks of the same charge, namely a kink-kink or antikink-antikink pair, it follows that there must be non-trivial dynamics. Take for instance the solution $N = 2$. In this case a field configuration of two kinks must satisfy the strict Bogomolny bound $E > 16$ because an equality attaining solution with this topological charge is not possible. However, when separating the two kinks infinitely wide apart, the energy will converge towards $E = 16$, the sum of two single kink solutions. Thus, there has to be a repulsive force between the two kinks. Analogously, we can argue for two antikinks. In fact, in the same manner as (12) was derived, it can be shown that for two kinks the interaction energy is given by

$$E_{int} = 32e^{-R},$$

where $R = 2a$.

Despite the fact that there are no static multi-kink solutions we can ask for what was not possible in the ϕ^4 -theory, namely analytical solutions in closed form of dynamic multi-kink scenarios. Maybe against one's expectations, the Sine-Gordon model in 1 dimension allows

the application of exact solution generating techniques such as the Bäcklund transformation. Using this powerful tool, it is indeed possible to find dynamical multi-kink solutions in closed form. Note that this characteristic is due to the fact that the Sine-Gordon model in 1 dimension is an integrable system. Partial differential equations belonging to this category are amongst others characterized by an infinite number of conserved quantities. Although further discussing the general properties of integrable systems is beyond the scope of this work, the application of the Bäcklund transformation is an important feature of Sine-Gordon and will be discussed in the following subsection.

4.2 Multi-kink solutions and Bäcklund transformation

With the goal of writing down analytical functions describing multi-kink interactions, we aim at using the Bäcklund transformation to investigate the behaviour of dynamical kinks in Sine-Gordon.

Given a solution of the equation of motion as a seed, the Bäcklund transformation generates a new solutions of this equation. It, therefore, maps between points in the solution space of the equation of motion.

It is convenient to switch to lightcone coordinates $x_{\pm} = \frac{1}{2}(x \pm t)$ and $\partial_{\pm} = \frac{\partial}{\partial x_{\pm}}$, so that the equation of motion of Sine-Gordon can be written as

$$\partial_- \partial_+ \phi = \sin \phi.$$

The Bäcklund transformation is then given by

$$\partial_+ \psi = \partial_+ \phi - 2\beta \sin \left(\frac{\phi + \psi}{2} \right), \quad \partial_- \psi = -\partial_- \phi + \frac{2}{\beta} \sin \left(\frac{\phi - \psi}{2} \right). \quad (14)$$

The Bäcklund parameter $\beta \in \mathbb{R} \setminus \{0\}$. These equations determine a function ψ which is again a valid solution of the Sine-Gordon field equations. Note here that the introduction of the Bäcklund parameter results in having a total of two free parameters, β and the integration constant a . Using the compatibility condition $\partial_- \partial_+ \psi = \partial_+ \partial_- \psi$ we get

$$\partial_- \partial_+ \phi - \beta(\partial_- \phi + \partial_- \psi) \cos \left(\frac{\phi + \psi}{2} \right) = -\partial_+ \partial_- \phi + \frac{1}{\beta}(\partial_+ \phi - \partial_+ \psi) \cos \left(\frac{\phi - \psi}{2} \right), \quad (15)$$

where we can insert the equations (14) to eliminate $\partial_- \psi$ and $-\partial_+ \psi$ on the left and the right side respectively. After some trivial simplifications and the use of the angle sum and difference identities for $\sin(\cdot)$ and $\cos(\cdot)$ equation (15) yields $\partial_- \partial_+ \phi = \sin \phi$. Analogously, the condition $\partial_- \partial_+ \phi = \partial_+ \partial_- \phi$ gives the same Sine-Gordon field equation for ψ . Therefore, we see that the Bäcklund transformation indeed maps between solutions. Given a seed (in this case ϕ), equation (14) generates a new solution to the same system introducing a new free parameter β .

A trivial example would be using $\phi = 0$ as a seed:

$$\partial_+ \psi = -2\beta \sin \left(\frac{\phi + \psi}{2} \right), \quad \partial_- \psi = \frac{2}{\beta} \sin \left(\frac{\phi - \psi}{2} \right).$$

These can be integrated given an ansatz of the form (13). The resulting function

$$\psi(x_+, x_-) = 4 \arctan(e^{-\beta x_+ - \frac{\beta}{x_-} + \alpha}), \quad (16)$$

where α is an integration constant, can be rewritten defining $v = \frac{1-\beta^2}{1+\beta^2}$, $\gamma = \frac{1}{\sqrt{1-v^2}} = \frac{-1-\beta^2}{2\beta}$ and $a = \frac{2\beta\alpha}{1+\beta^2}$:

$$\psi(t, x) = 4 \arctan(e^{\gamma(x-vt-a)}).$$

This is the dynamical single kink solution in the Sine-Gordon model.

A more involved case (calculation-wise) is the two-kink interaction. In that case, we start out with a seed solution $\psi_0 = 0$ and perform two Bäcklund transformations, one after the other, one with parameter β_1 and the other one with β_2 . This ensures that we can choose them so that the transformations yield two distinct field configurations ψ_1 (corresponding to β_1) and ψ_2 (corresponding to β_2). With the right choice of the Bäcklund parameters, the ψ_i describe two kinks at different positions in space moving towards each other. Taking these as new seed solutions, we now want to Bäcklund transform ψ_1 with β_2 and ψ_2 with β_1 . This step gives us ψ_{12} and ψ_{21} . The consistency condition $\psi_{12} = \psi_{21} = \psi_3$ allows to solve for ψ_3 analytically. To do so, we consider either the left or the right equation in (14), e.g.:

$$\begin{aligned}\partial_+ \psi_1 &= \partial_+ \psi_0 - 2\beta_1 \sin\left(\frac{\psi_0 + \psi_1}{2}\right) \\ \partial_+ \psi_2 &= \partial_+ \psi_0 - 2\beta_2 \sin\left(\frac{\psi_0 + \psi_2}{2}\right) \\ \partial_+ \psi_{12} &= \partial_+ \psi_1 - 2\beta_2 \sin\left(\frac{\psi_{12} + \psi_1}{2}\right) \\ \partial_+ \psi_{21} &= \partial_+ \psi_2 - 2\beta_1 \sin\left(\frac{\psi_{21} + \psi_2}{2}\right).\end{aligned}$$

This can be rewritten under the use of $\psi_{12} = \psi_{21} = \psi_3$ so that

$$\begin{aligned}\frac{1}{2}\partial_+(\psi_1 - \psi_0) &= -2\beta_1 \sin\left(\frac{\psi_0 + \psi_1}{2}\right) \\ \frac{1}{2}\partial_+(\psi_2 - \psi_0) &= -2\beta_2 \sin\left(\frac{\psi_0 + \psi_2}{2}\right) \\ \frac{1}{2}\partial_+(\psi_3 - \psi_1) &= -2\beta_2 \sin\left(\frac{\psi_3 + \psi_1}{2}\right) \\ \frac{1}{2}\partial_+(\psi_3 - \psi_2) &= -2\beta_1 \sin\left(\frac{\psi_3 + \psi_2}{2}\right).\end{aligned}$$

Now, we add/subtract the equations pair wise so that the derivatives drop out. Taking, for instance, equation 3 and subtracting 2, we obtain:

$$\begin{aligned}\frac{1}{2}\partial_+(\psi_3 - \psi_1 + \psi_0 - \psi_2) &= \\ 2\beta_2 \left[\sin\left(\frac{\psi_3 + \psi_1}{2}\right) - \sin\left(\frac{\psi_2 + \psi_0}{2}\right) \right] &= 2\beta_1 \left[\sin\left(\frac{\psi_3 + \psi_2}{2}\right) - \sin\left(\frac{\psi_1 + \psi_0}{2}\right) \right].\end{aligned}$$

Using $\sin(\alpha \pm \beta) = \sin(\alpha)\cos(\beta) \pm \cos(\alpha)\sin(\beta)$ as well as $\tan(\alpha \pm \beta) = \frac{\tan(\alpha) \pm \tan(\beta)}{1 \mp \tan(\alpha)\tan(\beta)}$, this simplifies to

$$\begin{aligned}\tan\left(\frac{\psi_3 - \psi_0}{4}\right) &= \frac{\beta_1 + \beta_2}{\beta_2 - \beta_1} \tan\left(\frac{\psi_1 - \psi_2}{4}\right) \\ \Rightarrow \psi_3 &= 4 \arctan\left[\left(\frac{\beta_1 + \beta_2}{\beta_2 - \beta_1}\right) \tan\left(\frac{\psi_1 - \psi_2}{4}\right)\right] - \psi_0.\end{aligned}\tag{17}$$

As described above, we set the initial seed solution $\psi_0 = 0$ so that ψ_3 describes the two-kink interaction. Given this, we can insert the single kink solution (16) of the form

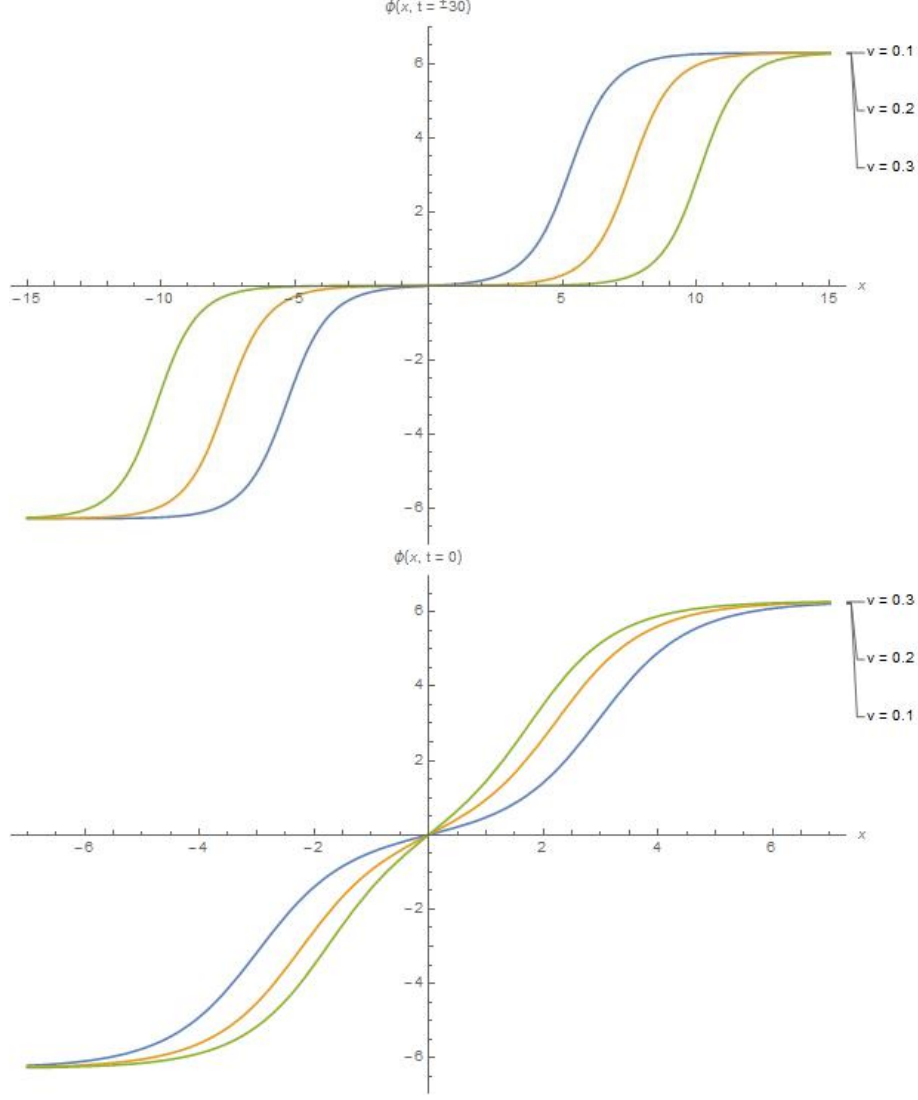


Figure 4: Equation (18) evaluated for $v = 0.1$ (blue), 0.2 (orange) and 0.3 (green) at $t = -30$ (upper plot), 0 (lower plot) and 30 (which takes exactly the same form as the upper plot) as a function of space x . $t = 0$ marks the time of closest approach.

$\psi_i = 4 \arctan(e^{\theta_i})$ with $\theta_i = -\beta_i x_+ - \frac{x_-}{\beta_i}$ for $i = 1, 2$. Note that α_i has been chosen to be zero. Then

$$\tan\left(\frac{\psi_1 - \psi_2}{4}\right) = \left(\frac{e^{\theta_1} - e^{\theta_2}}{1 + e^{\theta_1} e^{\theta_2}}\right) = \left(\frac{e^{\frac{\theta_1 - \theta_2}{2}} - e^{-\frac{\theta_1 - \theta_2}{2}}}{e^{-\frac{\theta_1 + \theta_2}{2}} + e^{\frac{\theta_1 + \theta_2}{2}}}\right) = \left(\frac{\sinh \frac{\theta_1 - \theta_2}{2}}{\cosh \frac{\theta_1 + \theta_2}{2}}\right).$$

For $\beta_1 = -\frac{1}{\beta_2} \equiv \beta$ and with the identifications made after equation (16) we finally find

$$\psi_3(t, x) = 4 \arctan \left[\frac{\beta - \frac{1}{\beta} \sinh(\gamma x)}{-\beta - \frac{1}{\beta} \cosh(\gamma vt)} \right] = 4 \arctan \left[v \frac{\sinh(\gamma x)}{\cosh(\gamma vt)} \right]. \quad (18)$$

This is a remarkable result since we have a functional description of a kink interaction. It is evident from figure 4 that the functions interpolate between -2π and 2π , hence, $N = 2$ and we see that the two kinks scatter of each other. Analyzing (18) for $|vt| \gg 1$ we see that indeed the the solution behaves like two separated kinks approaching each other until

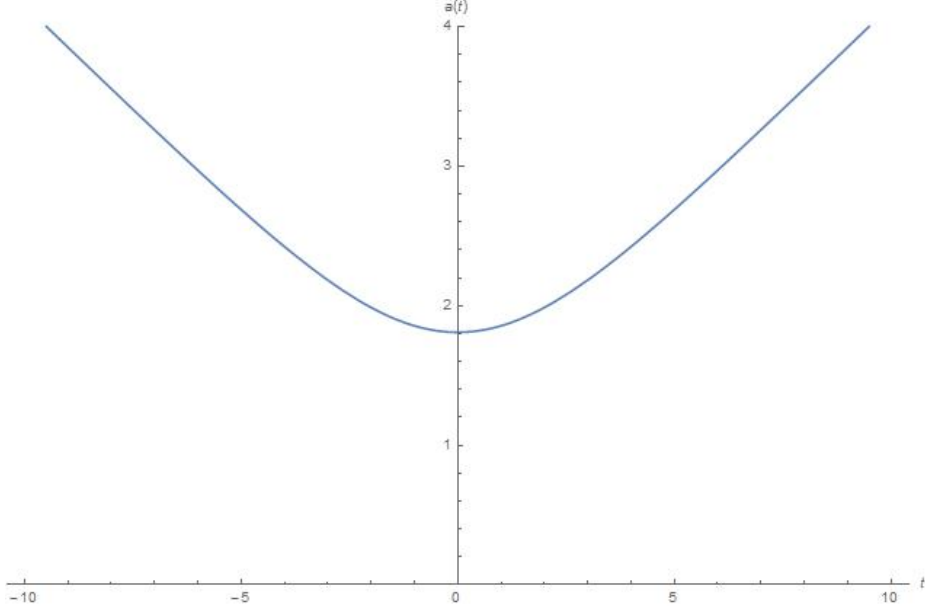


Figure 5: Equation (19) for $v = 0.3$ as a function of time t . $t = 0$ marks the time of closest approach. This trajectory indicates an elastic bounce as the kink-kink interaction since the separation trajectory is symmetric and never reaches zero.

the collision. For velocities much smaller than the speed of light ($v < 1$), at time $t = 0$ the two kinks reach minimal distance to each other and bounce off. The higher the velocity, the smaller this minimal distance (see 4). This gets even more evident as we rewrite (18) as

$$\psi(t, x) = 4 \arctan \left(\frac{(e^{\gamma x} - e^{-\gamma x})}{\frac{2}{v} \cosh(\gamma vt)} \right) = 4 \arctan(e^{\gamma(x-a)} - e^{-\gamma(x+a)}),$$

where we identified

$$a(t) = \frac{1}{\gamma} \log \left(\frac{2}{v} \cosh(\gamma vt) \right). \quad (19)$$

The two exponential functions resemble the two kinks at position $-a$ and a . Technically, the solution (18) is indistinguishable from a forward scattering with a shift of $2\delta = -2\frac{\log v}{\gamma}$. However, visualizing $a(t)$ in figure 5 and the fact that we argued for a repulsive force before gives strong evidence for backward scattering. The repulsive force alone makes backward scattering the more physical result.

We can continue the investigation and look for kink-antikink solutions in the Sine-Gordon model. One important feature of the Bäcklund transformation is that a solution of any N can be produced, given that the right seeds are chosen. For instance $N = 0$ can be produced via replacing $\psi_1 \rightarrow -\psi_1$ or equivalently $\psi_2 \rightarrow -\psi_2$ in (17). It is important to emphasize that the integrability of Sine-Gordon in this case prevents annihilation of kink and antikink and, instead, they scatter elastically. Intuitively, this can be understood using the feature of infinite number of conserved quantities. These fully characterise the solution asymptotically for $t < 0$, therefore imposing the same functional form asymptotically for $t > 0$ (after the scattering), thus, allowing only elastic scattering.

Furthermore, it is possible to adapt the initial speed and the distance in such a way that for $N = 0$, the solution is an exact time periodic bound state between kink and antikink, called breather.

This concludes the analytical analysis of the Sine-Gordon model. Before ending this chapter, we now turn to discussing the quantized topological charge of both models studied thus far. Since Sine-Gordon has a richer vacuum structure the following discussion will be based on this model.

4.3 Thirring-Model

We have seen that the Sine-Gordon model gives rise to topological charges $N \in \mathbb{Z}$. The corresponding topological current for the general Sine-Gordon ($\beta \neq 1$) can be constructed as:

$$j^\mu = \frac{\beta}{2\pi} \epsilon^{\mu\nu} \partial_\nu \phi.$$

This quantity is conserved independently of the equations of motion and is not associated to any symmetry of the Lagrangian. Most importantly, it takes discretized values although working in the classical regime.

A question one could ask now is if there is a quantum system which gives rise to the same current. Such an analogy would open up to more complicated questions about the connection of topological and Noether currents. And indeed such analogous quantum system exists.

The Thirring model is described by the Lagrangian

$$\mathcal{L} = \frac{1}{2} \bar{\psi} \gamma^\mu \partial_\mu \psi - \bar{\psi} \psi - \frac{1}{2} g \bar{\psi} \gamma^\mu \psi \bar{\psi} \gamma_\mu \psi,$$

where we work in 1+1-dimensional spacetime. γ^μ are the γ -matrices and ψ the fermi fields in 1+1-dimensional spacetime. This model admits a $U(1)$ -symmetry $\psi \rightarrow \psi' = e^{i\alpha} \psi$ which gives rise to the conserved Noether current $J^\mu = \bar{\gamma}^\mu \psi$ and the charge $Q = \int_{-\infty}^{\infty} J^0 dx$. Quantizing the theory results in similar quantities as in the Dirac field quantization. One of these is the commutator of the charge with the field $[Q, \psi] = -\hbar \psi$ which indicates that the charge is quantized in multiples of \hbar .

Both currents J^μ/\hbar and j^μ have charges within the spectrum \mathbb{Z} , yet the first is a Noether current the latter a topological one. However, quantizing the Sine-Gordon model takes the similarities even further when adjusting the free parameters of the model. Indeed, the currents become the same if we set

$$\frac{\beta^2 \hbar}{4\pi} = \frac{1}{\pi + g\hbar}.$$

Then, the algebras of the currents, which can be both written as

$$\begin{aligned} [j^0(x, t), j^0(y, t)] &= [j^1(x, t), j^1(y, t)] = 0 \\ [j^0(x, t), j^1(y, t)] &= iC \frac{\partial}{\partial x} \delta(x - y) \end{aligned}$$

coincide since for Sine-Gordon $C_{\text{Sine-Gordon}} = \frac{\beta^2 \hbar}{4\pi}$ while for the Thirring model $C_{\text{Thirring}} = \frac{1}{\pi + g\hbar}$. For the scalar field, we can just insert the definition of the topological current, calculate $\frac{\beta^2 \hbar}{4\pi} [\partial_1 \phi, \partial_0 \phi]$ and substitute in the definition of ϕ in the quantum regime as an integral over creation and annihilation operator $\phi(x) = \int \frac{dp}{2\pi 2e(p)} (a(p)e^{ipx} + a(p)^\dagger e^{-ipx})$. Then, we can just use the standard commutator relations. For ψ this calculation is much more involving. However, we can use $[Q, \psi] = -\hbar \psi$ to simplify the calculation.

Although this result is quite remarkable because it links classical topological and quantized Noether current, the relationship between ψ and ϕ is not trivial at all. One hint at this is that in the classical limit $\hbar \rightarrow 0$, $C_{\text{Sine-Gordon}} \rightarrow 0$ while $C_{\text{Thirring}} \neq 0$.

The relation between these two models is actually much richer than just their current commutator algebra. For this work, however, it is enough to point out the importance of topologically non-trivial vacua. The duality of the currents between Sine-Gordon and Thirring was introduced to show how the topological structure of the vacuum could be related to symmetries or even gauge symmetries of field theories in different regimes. An exhaustive characterisation of such analogies remains an open question and should motivate the reader to further investigate. This underlines the potential for interesting applications of kinks or solitons in general in quantum field theory.

5 Simulations

So far, we derived analytical results of Sine-Gordon and ϕ^4 -theory often with intuitive explanations of what happens a later times especially in the multi-kink scenarios. As mentioned in the introduction, we will now describe a framework to approach these models numerically and simulate the multi-kink interactions. These simulations confirm quantitatively what was intuitively explained.

5.1 General approach

Simulating the kink solutions generally means that we need to simulate the Klein-Gordon equation since it determines the dynamics through its equation of motion. The Klein-Gordon is a partial differential equation of second order which makes it numerically challenging to simulate. In this work we approach this problem via an implicit-explicit (IMEX) time stepping scheme, following Donninger and Schlag [4], meaning that we use the current state and an older state (state at earlier times) together to calculate the future state of the system. This is a common technique in numerical simulations and it is convenient to choose a degree three discretization such that the field ϕ splits into ϕ_{new} , $\phi_{current}$ and ϕ_{old} . The important feature of this method is that the IMEX-stepping scheme describe above approximately preserves energy [5], although time is discretized into small steps. This is especially important given that kinks are minimal energy solutions for a given topological class of field configurations. Thus, the outcome of interaction processes heavily relies on the principle of energy conservation.

Having a look at the equation of motion

$$\frac{\partial^2}{\partial t^2}\phi - \nabla^2\phi = \frac{dU}{d\phi},$$

we not only encounter time but also spacial derivatives. As mentioned, the time derivatives are handled via the time scheme stepping, requiring the discretization of time in small steps δt . For the spacial derivatives we want to use Fourier transform to execute the calculations. To be more accurate, we use *fast Fourier transform*, a numerical implementation of a discrete Fourier transform $A_k = \sum_{m=0}^{n-1} a_m e^{-2\pi i \frac{mk}{n}}$ which deconstructs a function into its Fourier coefficients a_m time efficiently (which was brought to light in its current form by Cooley and Tukey [6]). Therefore, the calculation of the spatial derivatives will be executed in Fourier space. Over all, the code, whose steps we will then proceed into detail further, will have the following structure:

1. Define the equation of motion at $t = t_{min}$. Discretize the field using ϕ_{new} , $\phi_{current}$ and ϕ_{old} , where the time distance between each is δt : Starting from the general equation of motion as stated at the beginning of this chapter we, first, want to introduce a degree three discretization. To do so, we transform the field ϕ in the following form:

$$\phi \rightarrow \frac{1}{2} \left(\frac{\phi_{n+1} + \phi_n}{2} + \frac{\phi_n + \phi_{n-1}}{2} \right) = \frac{\phi_{n+1} + 2\phi_n + \phi_{n-1}}{4}$$

Here, we slightly changed the notation to $\phi_{old} \equiv \phi_{n-1}$, $\phi_{current} \equiv \phi_n$ and so on. For the time derivative we apply twice

$$\frac{d\phi(t, x)}{dt} = \lim_{\delta t \rightarrow 0} \frac{\phi(t + \delta t, x) - \phi(t, x)}{\delta t} = \lim_{\delta t \rightarrow 0} \frac{\phi_{n+1} - \phi_n}{\delta t},$$

so that the derivative term reads $\frac{\partial^2}{\partial t^2}\phi \rightarrow \frac{\frac{\phi_{n+2}-\phi_n}{\delta t} - \frac{\phi_n-\phi_{n-1}}{\delta t}}{\delta t}$. All in all, the equation of motion transforms into

$$\frac{\phi_{n+1} - 2\phi_n + \phi_{n-1}}{(\delta t)^2} - \nabla^2 \frac{\phi_{n+1} + 2\phi_n + \phi_{n-1}}{4} = \frac{dU}{d\phi}. \quad (20)$$

For the term on the r.h.s., we apply the same scheme as for the single fields after calculating the derivative explicitly. Nonlinear terms in this expression are treated separately and for now are left as they are.

2. For every time step with in the interval of interest $[t_{min}, t_{max}]$ do:

2.1. Apply fast Fourier transform to the equation of motion with discretized fields: This can be done term by term and we just replace $\phi \rightarrow \tilde{\phi}$ and $\nabla^2 \rightarrow k^2$, where k is the momentum. However, if $\frac{dU}{d\phi}$ contains non-linear terms in ϕ , such as ϕ^3 in the ϕ^4 -theory or $\sin(\phi)$ in the Sine-Gordon model, they are simply Fourier transformed separately, not using degree three discretization.

2.2. Solve the Fourier transformed equation of the three transformed fields $\tilde{\phi}_{new}$, $\tilde{\phi}_{current}$ and $\tilde{\phi}_{old}$ with respect to $\tilde{\phi}_{new}$:

We solve for $\tilde{\phi}_{n+1}$ after Fourier transforming equation (20) and get, after some simple math, (in the case of the ϕ^4 -potential with $\lambda = \frac{1}{2}$ and $m = 1$)

$$\tilde{\phi}_{n+1} = \frac{1}{\frac{1}{(\delta t)^2 - \frac{k^2}{4} - \frac{1}{2}}} \left[\frac{1}{2}(2\tilde{\phi}_n + \tilde{\phi}_{n-1}) + k^2 \frac{2\tilde{\phi}_n - \tilde{\phi}_{n-1}}{4} - 2(\tilde{\phi}_n)^3 + \frac{1}{(\delta t)^2}(2\tilde{\phi}_n - \tilde{\phi}_{n-1}) \right]. \quad (21)$$

As it is shown here, $(\tilde{\phi}_n)^3$ represents the Fourier transform of $(\phi_n)^3$. There is no discretization applied in this case. The equations like (21) are exactly what has to be done analytically and implemented into the program by hand for each model. They govern the numerical evolution of a chosen field configuration.

2.3. Use the *inverse fast Fourier transform* in order to get the solution for the defining field ϕ_{new} in position space.

2.4. Save the result ϕ_{new} in a list. Set $\phi_{old} = \phi_{current}$ and $\phi_{current} = \phi_{new}$.

2.5. Set the time to be $t = t + \delta t$. Check if $t < t_{max}$, if so, jump back to 2.1., otherwise end the loop and continue with step 3..

3. Display the list that contains the time evolution of ϕ .

We implemented the scheme above in PYTHON and made it available at <https://github.com/maibachd/kinksnumerics> [7]. In this repository, there are a number of simulations, animations and thoroughly commented code examples for the ϕ^4 as well as the Sine-Gordon model. Since this work cannot include any animation of simulations of dynamical kink solutions we invite the reader to visit the website and convince themselves of the accuracy of the analytical results. The data file `Readme.md` contains further instruction about how to navigate through this repository.

5.2 Multi-kink interaction

One of the animations that can be found in ref. [7] is the annihilation of a kink and antikink in the ϕ^4 -model. As we discussed in section 3, there is no analytical solution for this scenario. The only analytically approximated result was for the interaction force. This result, however, only holds asymptotically, meaning for large separation of kink and antikink.

Based on this we can construct a differential equation for their separation and compare this result to the exact one, from the numerical simulation of the program, as done in `kink-antikink-attraction-in-phi4.gif` in ref. [7].

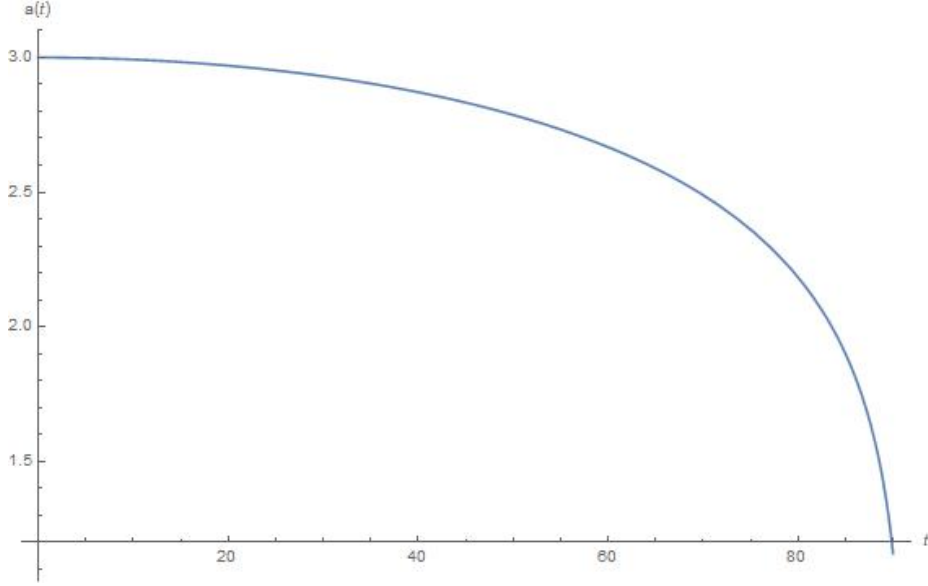


Figure 6: Equation (22) for $a_0 = 3$ as a function of time t . At $t \approx 85$ kink and antikink collide.

The differential equation simply results from Newton's law $F = M\ddot{x}$ where the mass for kink or antikink equivalently was given by the Bogomolny bound in equation (8). Choosing $\lambda = \frac{1}{2}$ and $m = 1$ the rest mass of the kink or antikink is set to $M = \frac{4}{3}$. The differential equation then reads:

$$\frac{4}{3}\ddot{a}(t) = -32e^{-4a(t)},$$

where the $-$ sign in front of the force comes from the fact that we consider the kink and antikink approaching $x = 0$.

With the initial conditions $\dot{a}(0) = 0$ and $a(0) = a_0$ we can use a symbolic calculation program such as MATHEMATICA to solve this differential equation. One result in this case would be

$$a(t) = \frac{1}{2} \log \left[\frac{\sinh \left(4\sqrt{-3}e^{-4a_0} \left(\frac{1}{8\sqrt{3}}e^{2a_0}\pi + t \right) \right)}{\sqrt{-e^{-4a_0}}} \right]. \quad (22)$$

Since the evaluation clearly requires complex calculations which are not easy to implement in Python, we print out a table with values for all the time steps δt between $[t_{min}, t_{max}]$ in Mathematica and use it as an interpolation table the Python code (see `KKequ-two-kink.py` in [7]). The trajectory is visualized in figure 6.

Note that this construction is not necessary for the Sine-Gordon model since the Bäcklund transformation allows us to get exact analytical solutions in a closed form even for the multi-kink scenario.

So far, this concludes the description of the numerical part of this work. For more insights and the actual code, we refer the reader to ref. [7].

6 Conclusion

We summarize here the main findings of studying analytical results of the ϕ^4 - and the Sine-Gordon model.

In section 4 we compared a model in the quantum regime, the Thirring model, with our classical Sine-Gordon model and found that, given the free parameters of the theories are adapted adequately, the topological current of Sine-Gordon coincides with the Noether current corresponding to the $U(1)$ symmetry of the Thirring model. This hints at a correspondence between topology and gauge theories and the potential of such bridges between the topology of vacuum manifolds of classical field theories and symmetries of systems from quantum field theory is not fully explored yet.

Performing numerical simulations as described in section 5 and analyzing the results (see [7]), we see that the time stepping scheme combined with the degree three discretization allows accurate numerical simulations of the Klein-Gordon equation. In fact the relative error is of order $10^{-4} - 10^{-3}$ which is very good given the relatively simple simulation procedure. It is worth mentioning that the programs in ref. [7] are generally constructed in such a way that arbitrary scalar potential for a 1-dimensional real field could be implemented with minimal effort. Moreover, it is possible that a similar procedure would also work for the generalization of kinks in higher dimensional spacetime.

All in all, it is worth investigating topological structures of classical field theories, if it may be numerically or analytically. After all, these structures appear everywhere in physics, as discussed in section 1, and their understanding can lead to deeper insights into quantum field theories.

A Topology and vacuum manifolds

We will briefly define the background knowledge and notation required to study solitons, especially kinks in 1+1-dimensional space time. For this we follow chapter 3 and 4 of [1].

Define two manifolds X and Y without boundaries. A continuous map Ψ can be defined by $\Psi : X \rightarrow Y$, where we identify a base point $x_0 \in X$ which is mapped onto $y_0 \in Y$. If such base point exist, Ψ is called a based map.

Two based maps Ψ_0 and Ψ_1 are said to be homotopic to each other if we can continuously deform one into another by the means of a continuous map $\tilde{\Psi} : X \times [0, 1] \rightarrow Y$. Here, we parametrized $\tau \in [0, 1]$ such that $\tilde{\Psi}|_{\tau=0} = \Psi_0$ and $\tilde{\Psi}|_{\tau=1} = \Psi_1$. Since *homotopic* is an equivalence relation we can classify maps Ψ into homotopy classes. One instance of such would be the constant class consisting of $\Psi(x) = y_0$.

Specifying X allows us to characterize the homotopy classes further. Consider X to be the n -sphere S^n . The set of homotopy classes based on $\Psi : S^n \rightarrow Y$ is defined as $\pi_n(Y)$ for $n \geq 0$. The set $\pi_n(Y)$ forms a group called the n th homotopy group of Y .

Since the treatment of $n \geq 1$ is not required in this work, we will stop here the formal introduction into homotopy theory here and directly address the application to vacuum manifolds.

For what consider n classical static scalar fields $\phi = (\phi_1, \dots, \phi_n)$ with energy given by

$$E = \int \left(\frac{1}{2} (\nabla \phi_i)^2 + U(\phi_1, \dots, \phi_n) \right) d^d x$$

in d dimensions. Let $\mathcal{V} \in \mathbb{R}^n$ describe the submanifold where $U = U_{min} = 0$, namely the vacuum manifold of the theory. There is no constraint on finite points \vec{x} but at spacial infinity the energy density has to vanish in order to implement finite energy boundary conditions. Hence, ϕ at spatial infinity must be an element of \mathcal{V} . A field configuration can, thus, be defined as a map from the edges of the n -Sphere, namely the sphere at infinity in \mathbb{R}^{n+1} , into \mathcal{V} , where $n = d - 1$. The only topologically relevant information is implicitly given by the map

$$\phi^\infty : S_\infty^{d-1} \rightarrow \mathcal{V}.$$

As this maps two manifolds, we can assign different maps ϕ_i^∞ that describe possible field configuration to their corresponding homotopy class. If two maps $\phi_i^\infty, \phi_j^\infty$ are within the same homotopy class they describe the same physical scenario. Hence, the topological character of field configuration is classified by the homotopy class of ϕ^∞ , which is an element of $\pi_{d-1}(\mathcal{V})$.

For the cases of interest of this work, $d = 1$ and $\phi^\infty : S_\infty^0 \rightarrow \mathcal{V}$. S_∞^0 consists of $\pm\infty \in \mathbb{R}$, thus, we map two points into the vacuum manifold \mathcal{V} considered. In this simple case, the homotopy class $\pi_0(\mathcal{C})$ divides \mathcal{V} into topologically distinct vacua. The topological class of a field is then given by the element $\pi_0(\mathcal{V}) \times \pi_0(\mathcal{V})$. To get field configurations with distinct topological data, it thus needs a vacuum manifold \mathcal{V} with at least two topologically distinct vacua. Furthermore, solitons can only exist if we have more than two topologically distinct elements in the vacuum manifold which is equivalent to demanding $\pi_0(\mathcal{V})$ to be non-trivial. As an clarifying example consider figure 7. The left potential has only one element in $\pi_0(\mathcal{V})$ since every map to a any value of the vacuum manifold $\mathcal{V} = [-1, 1]$ can be continuously deformed to $\phi = 0 \in \mathcal{V}$, while the right potential has two elements. There is no map continuously connecting these points without leaving the vacuum manifold, hence, they are topologically protected and solitons can arise.

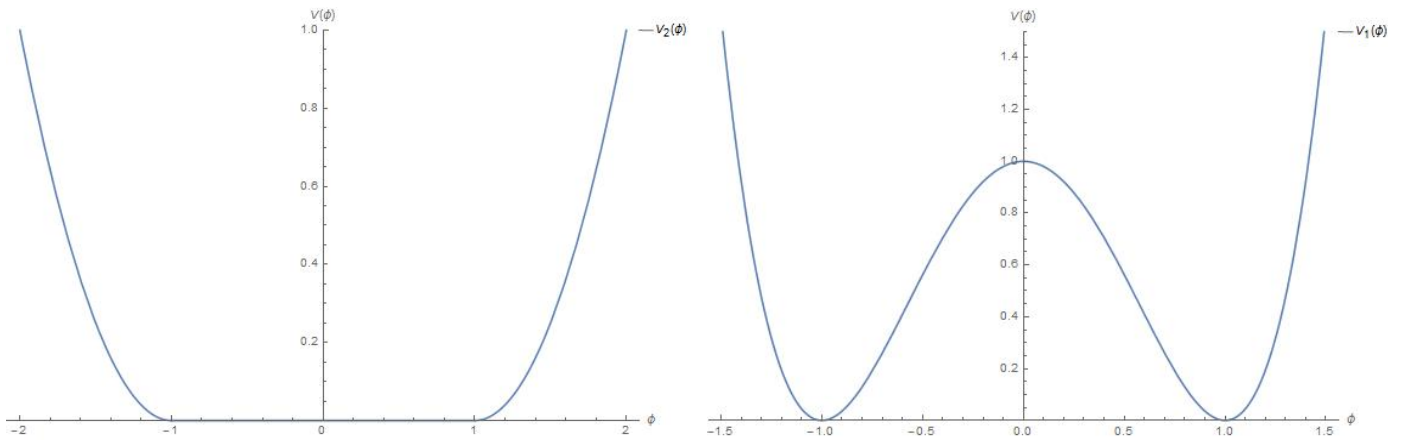


Figure 7: Two possible potentials as functions of ϕ . V_1 has two degenerated but topological distinct vacua while for V_2 all points in the vacuum manifold are topologically indistinguishable and the topology class $\pi_0(\mathcal{V}_2)$ is trivial.

References

- [1] N. Manton and P. Sutcliffe, *Topological solitons*. Cambridge University Press, 2004.
- [2] A. R. Gomes, F. C. Simas, K. Z. Nobrega, and P. P. Avelino, “False vacuum decay in kink scattering,” *arXiv preprint arXiv:1805.00991*, 2018.
- [3] P. Goddard and D. Olive, “Magnetic monopoles in gauge field theories,” *Rep. Prog. Phys.*, vol. 41, p. 1357, 1978.
- [4] R. Donninger and W. Schlag, “Numerical study of the blowup/global existence dichotomy for the focusing cubic nonlinear klein-gordon equation,” *Nonlinearity*, vol. 24, pp. 2547–2562, 2011.
- [5] R. LeVeque, *Numerical Methods for Conservation Laws*. Springer, 2012.
- [6] J. W. Cooley and J. W. Tukey, “An algorithm for the machine calculation of complex fourier series,” *Math. Comput.*, vol. 19, pp. 297–301, 1965.
- [7] D. Maibach. (2020) Git repository: kink/numerics. [Online]. Available: <https://github.com/maibachd/kinksnumerics>